Biomaterials Science

Surface modification of strontium-doped porous bioactive ceramic scaffolds via poly(DOPA) coating and immobilizing silk fibroin for excellent angiogenic and osteogenic property

Journal:	*Biomaterials Science*
Manuscript ID	BM-ART-10-2015-000482.R1
Article Type:	Paper
Date Submitted by the Author:	12-Jan-2016

Complete List of Authors:	Wang, Xu; College of Polymer Science and Engineering, Gu, Zhipeng; West China Hospital, Sichuan University, Department of Neurosurgery Jiang, Bo; College of Chemistry, Li, Li; the 452 Hospital of Chinese PLA, Department of Oncology Yu, Xixun; Sichuan University, polymer science and engineering

Journal Name ARTICLE

Surface modification of strontium-doped porous bioactive ceramic scaffolds via poly(DOPA) coating and immobilizing silk fibroin for excellent angiogenic and osteogenic property

Received 00th January 20xx,
Accepted 00th January 20xx

DOI: 10.1039/x0xx00000x

www.rsc.org/

Keywords:

Dopamine, Strontium-doped, calcium polyphosphate (SCPP), interfacial compatibility, angiogenic growth factors, silk fibroin (SF)

Xu Wang[a.#], Zhipeng Gu[b.#], Bo Jiang[c], Li Li[d],and Xixun Yu[a]*

For bioceramic scaffolds employed in clinical applications, excellent bioactivity and tenacity were of great importance. Modifying inorganic SCPP scaffolds with biological macromolecules could obviously improve its bioactivity and eliminate its palpable brittleness. However, it was hard to execute directly due to extremely bad interfacial compatibility between them. In this research, dopamine (DOPA) was introduced onto strontium-doped calcium polyphosphate (SCPP) scaffolds, subsequently the preliminary material was successfully further modified by silk fibroin (SF). SCPP/D/SF possessed suitable biomechanical properties, ability to stimulate angiogenic factors secretion and excellent biocompatibility. Biomechanical examination demonstrated SCPP/D/SF scaffolds yielded better compressive strength because of improved interfacial compatibility. MTT assay and CLSM observation showed that SCPP/D/SF scaffolds had good cytocompatibility and presented better inducing-cells-migration potential than pure SCPP scaffolds. Meanwhile, its ability to stimulate angiogenic factors secretion was measured through ELISA assay and immunohistological analysis in vitro and vivo respectively. The result revealed, superior to SCPP, SCPP/D/SF could effectively promote VEGF and bFGF expression, possibly leading to enhancing angiogenesis and osteogenesis. In a word, SCPP/D/SF could serve as a potential bone tissue engineering scaffold for comparable biomechanical and excellent bioactivity. It provided a novel idea for inorganic material's modification to prepare the promising bone tissue engineering scaffold with ability to accelerate bone regeneration and vascularization.

1 Introduction

Biomaterials play a critical role in clinical applications to heal bone defects and reconstruct bone tissues[1]. Some traditional bone repairing materials such as hydroxyapatite (HA) and tricalcium phosphates (TCP) have been used clinically. However, their undegradation or uncontrollable degradation has emerged as the main problem. Besieds, their low toughness and lack of osteogenic properties also limited their further application. SCPP, a bioactive ceramic possesses similar mineral component with bone, has drawn inclusive attention for its comparable physicochemical properties, controllable degradability and excellent biocompatibility. Popularly, SCPP was employed in bone defects regeneration, which was attributed to its controllable degradation rates, remarkable osteoconductivity, low cytotoxicity and some bioactivity in stimulating angiogenesis[2-4]. Nevertheless, similar to other inorganic materials, further applications are limited by its palpable brittleness and low compressive strength, which may lead to insufficient ability for higher-load bearing bone repair[5]. Therefore, to eliminate its brittleness and to further improved its bioactivity, SCPP scaffolds should be chemically modified by organic biological macromolecules.

Among naturally derived biopolymers, SF was an ideal macromolecule agent for chemical modification of inorganic materials used in bone regeneration, owning to its remarkable toughness, controllable degradation, limited inflammatory potential, obvious promotable cell adhesion and proliferation, as well as high bioactivity to stimulate angiogenic growth factors secretion.[6-9] However, extremely bad interfacial compatibility between SF and inorganic materials made it difficult to form stable modification structure through SCPP/SF materials interface. Conventional methods to prepare organic-inorganic composite materials mainly contained simply physical mixing and chemical fixing by crosslinking reagent. But physical mixings always lead appearance of serious phase separation resulting from extraordinary instability between organic-inorganic interface.[10, 11] Meanwhile, crosslinking reagent can only fix inorganic phase via forming network structure with SF, which shows poor incorporation as well[12-14]. To address this problem, miraculous biomolecule DOPA was coated to modify SCPP surface to immobilize third-party organic biomaterials[15-17]. The modification of scaffolds by DOPA has attracted more and more attentions in biomaterial applications for easy operation, solvent-free, non-toxic and excellent adherent property[18, 19]. Superior to above, through self-polymerization, DOPA could form surface-adherent films onto great majority of materials including metals, polymers, semiconductors and ceramics. It can be inferred that DOPA modified organic-inorganic composite scaffolds would be much more stable to eliminate serious phase separation. DOPA has been certified to be ideal adhesion molecules for modifying the surface of many biomaterials. It was employed in coating synthetic polymer materials to enhance the affinity between cells and substrates, and could also be used as a versatile affinity tag for immobilizing proteins on biomaterials. Recently, to accomplish surface heparinization, Zhu et al.

[a.] College of Polymer Science and Engineering, Sichuan University, Chengdu 610065, P.R. China.
[b.] Department of Neurosurgery, West China Hospital, Sichuan University, Chengdu 610065, P.R. China
[c.] College of Chemistry, Sichuan University, Chengdu 610065, P.R. China.
[d.] Department of Oncology, the 452 Hospital of Chinese PLA, Chengdu, Sichuan Province 610021, P.R. China
 # These authors contributed equally.
Corresponding Email: yuxixun@163.com

introduced DOPA to coat poly (vinylidene fluoride) (PVDF) and covalently immobilized heparin onto it[20-23]. This modification effectively improved the hemocompatibility and mechanical properties of materials. Nevertheless, there were still no reports about using DOPA as adhesion molecules to modify the surface of inorganic materials to enhance organic -inorganic interface compatibility of the organic-inorganic composite scaffolds in present studies.

In this study, DOPA was introduced to coat the surface of porous SCPP as intermediary agent. Firstly, the adjacent hydroxyl groups in DOPA molecule could spontaneously oxidative-polymerize to form strongly adherent film for conjugation of SCPP scaffolds; Secondly, an easy reaction between oxidized phenolic hydroxyl (quinone) and amines on SF can covalently immobilize SF inside the porous inorganic SCPP scaffolds. This facile two-step DOPA-surface modification not only completely eliminated its brittleness, but also further improved its bioactivity. With ability to induce new bone formation and to stimulate angiogenesis, the SCPP/D/SF composite scaffolds could be potential materials for bone tissue-engineering.

2 Materials and experimental

2.1 Surface modification of SCPP scaffolds

Porous SCPP scaffolds (with Ca/Sr molar ratio of 92:8, 10 mm in diameter, 2 mm in thickness) were prepared as previously reported methods and employed as original materials.[3] Meanwhile, a 2.0 mg/mL DOPA solution was prepared by dissolving dopamine (Sigma Company, USA) in Tris-HCl buffer solution (10 mM, PH 8.5)[22]. To accomplish primary modification, the SCPP samples were immersed into 20mL DOPA solution for 7 h with continuous shaken (this favorable reaction condition was selected through measuring their amino concentration in **Figure S1**). Subsequently, specimens were taken out and rinsed with deionized water to remove physically adsorbed DOPA, giving a DOPA-coated SCPP scaffolds (D-SCPP). After being dried at 40 °C to constant weight, silk fibroin (SF with β-sheet structure was employed and it was extracted from bombyx morisilk) was employed to further modify D-SCPP. Analogously, the intermediate scaffolds were immersed in 10 mg/ml SF/Tris-HCl buffer solution for 24 h under vacuum condition to form the SCPP-DOPA-SF (SCPP/D/SF) composite scaffolds. After redundant SF being washed out entirely, the ultimate scaffolds were successfully prepared. As control group, GA-fixed samples were also prepared in this research. The chemical compositions distributed on the surface of composite scaffolds were analyzed by X-ray photoelectron spectroscopy (XPS, PHI 5000C ESCA System) with Al Kα excitation radiation (1486.6 eV).

2.2 Scaffold characterization

To determine mechanical-property changes of modified scaffolds caused by SF, the compressive strength of column shaped sample was detected by electronic mechanical testing machine (Instron 4302, USA) at a constant speed of 2.0 mm/min and its compressive strength was calculated from measured load and cross sectional area. The cross section morphologies of treated scaffolds were examined by SEM (JSM-5900LV, JEOL, Japan). Additionally, a Charpy-type impact tester was used to determine the impact strength and its impacted surface was observed by SEM. Subsequently, the qualitative chemical composition of different regions in scaffolds were analysed by scanning electron microscope–X-ray energy dispersion spectrum (SEM-EDS) with accelerating voltage of 20 kV with Oxford spectrometer.

2.3 Molecular dynamics simulation

Typically, molecular dynamics simulation was performed to predict the reaction mechanism between DOPA and inorganic materials. In this research, CPP crystal lattice simulation was used as model of SCPP's since Sr possessed similar atomic structure to Ca. The original crystallographic structure of calcium polyphosphate (CPP) was derived from CCDC database in Cambridge. After being optimized by Forcite plus (lattice parameter: a=14.6552Å, b=16.2564Å, c=9.7632Å), NVT dynamic model was employed in this research and an individual DOPA molecule was embedded in any possible position in CPP crystal lattice. As previously reported DOPA molecule contacted with CPP mainly through catechol or quinone groups, thus the designed simulation box includes a CPP slab in its bottom surface and an adsorbed DOPA molecule above. Subsequently, the orbit of DOPA on CPP was obtained in molecular dynamics simulation.

2.4 Proliferation of HUVECs or MG63 seeded on scaffolds

In this study, Human Umbilical Vein Endothelial Cells (HUVECs) and human osteosarcoma cell line (MG63) purchased from West China Hospital, Sichuan University were chosen to investigate the cytocompatibility of SCPP/D/SF scaffolds. After all scaffolds had been sterilized by gamma irradiation, they were placed to the bottom of wells in 24-well plate (n=4) and immersed in culture medium for 12 h. Once cells reached passage three, they were trypsinized to to be detached[24]. Subsequently, fresh DMEM culture medium supplemented with 10% fetal bovine serum (BCS), 100 U/ml penicillin and 100 mg/ml streptomycin (Gibcobrl, Grand Island, NY, USA) were added to create cell suspension with predetermined density. Then 500 μL DMEM growth medium suspensions of HUVECs at 3×104 cell/ml and/or that of MG63 at 5×104 cell/ml were seeded onto corresponding wells, respectively. The incubation was carried out under suitable condition (5% CO_2, 37 °C) for 6 days and the culture medium were refreshed every two days. MTT assay was employed to assess cell proliferation. On the 2, 4 and 6 day, 60 μL/well of MTT solution (5 mg/ml in phosphate buffered saline, PBS) was added and 4 h further incubation was carried on to make formazan crystallized completely. Then liquid in wells was sucked off, and 400 μL/well dimethylsulfoxide (DMSO) was added, followed by constantly shaking for 10 min to dissolve formazan crystals completely. The optical density (OD) value of this solution was measured at 492 nm with a Microplate Reader (Model 550, Bio Rad Corp.).

2.5 CLSM examination

Confocal laser scanning microscopy (CLSM), combined with fluorophore, provided us a lever to detect the three-dimensional architecture of scaffolds and to observe cells distribution inside its pores. Briefly, HUVECs and MG63 were seeded onto scaffolds respectively at a density of 2.5×104 cells/well in 24-well plate. After incubating for 3 days, samples were washed with PBS for three times to remove unattached cells and then immersed in fluorescein isothiocyanate solution (FITC; Sigma; diluted with DMEM to 10ug/ml) for another 2h to dye their cytoskeleton[25]. Afterwards, the washed samples were fixed using 4% paraformaldehyde 30 min and then 200 µl of 4, 6-diamino-2-phenylindole (DAPI, 10µg/ml) was added to label its cell nucleus for 10 min[26]. Ultimately, the stained samples were photographed by confocal laser scanning microscopy (CLSM).

2.6 Alkaline phosphatase (ALP) activity and mineralization analysis

Cells were seeded onto scaffolds at a density of 5×10^4 cells/well and cultured for predetermined time (4 d, 7 d, 10 d, and 14 d, respectively). Then, scaffolds were washed twice with PBS. Cells were lysed by 0.1% Triton X-100. After centrifugation at 2000 rpm for 20 min, the supernatants of cell lysate solutions were collected. Together with supernatant of culture medium, ALP activity was determined by measuring absorbance with a Microplate Reader (Model 550, Bio Rad Corp.) at 405 nm. To observe the mineralized matrix, cells adherent to scaffolds were fixed with 95% ethanol for 15min[27]. Then mineralization was observed under light microscope after it was incubated in a solution containing 1% alizarin red and 1% ammonium hydroxide at 37 °C for half an hour.

2.7 Measurement of VEGF and bFGF protein secretion

The protein secretion of VEGF and bFGF was evaluated by double ligand enzyme-linked immunosorbent assay (ELISA). After these scaffold samples were co-cultured with HUVECs and/or MG63 for 7 days, supernatant liquid for ELISA assay was collected through centrifugation at 14000 rpm for 5 minutes. According to Kit instructions (R&D Corp.), the concentrations of VEGF and bFGF were accurately determined and their values were expressed as pg/ml.

2.8 Vivo implantation and histological observation

Thirty-six healthy New Zealand white rabbits weighing 2.5±0.4 kg were randomly assigned to nine groups. All experimental animals were cared according to guidelines formulated by National Institutes of Health guidelines on the humane, and all procedures performed on animals were approved by Animal Care and Use Committee of Sichuan University. After rabbits were anesthetized using pentobarbital sodium under aseptic conditions, a longitudinal incision was made on their skulls to expose the bone surface. Subsequently, the periosteum on bone surface was separated and removed, and the crinial bone was bored to form 10 mm diameter bone defect on calvaria. Once defects were created, SCPP, D-SCPP and SCPP/D/SF scaffolds with dimensions of Φ10mm×2mm were carefully implanted into into defects. All rabbits were euthanized after being implanted for predetermined period (4, 8 and 12 weeks, respectively) and those scaffolds with surrounding tissues were collected. Being fixed in 10% formalin for 2 days, the excised specimens were adequately decalcified in EDTA solution (pH8.0, 0.5 M) for histological observation. These decalcified bones were embedded in paraffin and sectioned into 5µm-thickness sections for hematoxylin and eosin (HE) staining[28]. Immunohistological procedures were carried out as a modifie method reported by Kon et al[29,30]. Briefly, 3% hydrogen peroxide was added and incubated for 10min to extinguish endogenous peroxidase activity. Sections were immersed in 1mM EDTA solution boiled by high temperature steam for 1min to unmask antigen and then incubated with anti-VEGF or anti-bFGF (anti-rabbit, Beijing Zhong Shan Golden Bridge Biological Technology CO., China) for 1 h at room temperature. Secondary labeling was accomplished by incubating with appropriate biotin-conjugated secondary antibody and streptavidin-peroxidase for 10 min, respectively. Ultimately, color was developed by immersing the pretreated sections in fresh DAB solution for up to 3 min, and the color development was investigated under optical microscope.

2.9 Statistical Analysis

Staistical analysis was performed by SPSS 13.0 (Statistical Product and Service Solutions, Version 16.0, SPSS Inc. Chicago IL, USA). Experimental data was depicted as means ± standard deviation (SD). To determine the differences in measured properties of parallel experimental groups, it was performed with one-way analysis of variance (one-way ANOVA) for statistical significant, and differences were considered significant if $p < 0.05$.

3. Results and Discussion

In aqueous solution, partial DOPA can be easily oxidized into DOPA o-quinone. The reverse dismutation reaction between this oxidation mediate and its relatively reducing original

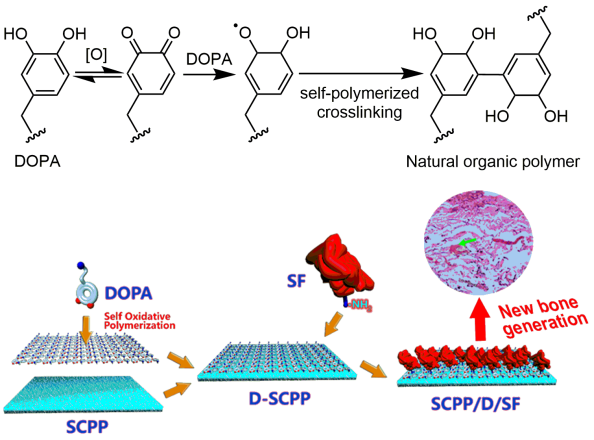

Scheme.1 Mechanism of two-step modification of SCPP porous scaffold with DOPA and SF in succession

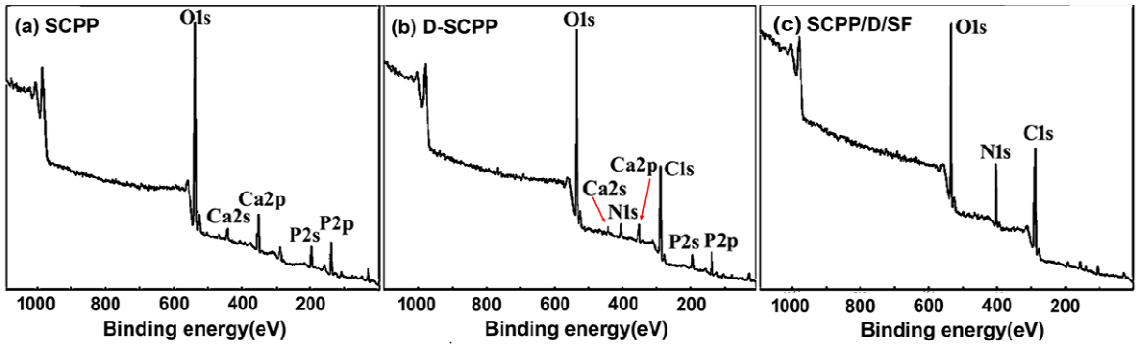

Fig.1 XPS analysis of SCPP, D-SCPP and SCPP/D/SF scaffolds

reactant immediately resulted in self-polymerized crosslinking structure on the material interface. Such a thin polymer layer very tightly adhered to the surface of scaffolds, making it stable enough to prevent being peeled off, unless soaking in strong acid/alkali or proceeding with ultrasonic concussion [19]. DOPA endowed inorganic SCPP scaffolds (D-SCPP) had excellent biocompatibility. With quantities of catechol groups, it could easily bond with active amino groups on SF molecular chains. Ultimately, SF could be covalently immobilized onto the D-SCPP scaffold. It not only further improved the biocompatibility of composite scaffolds but also successfully eliminated the fragility of inorganic ceramic material.

3.1 XPS for surface compositions

The effect of two-step DOPA-modification on SCPP scaffold was ascertained by XPS through comparing the surface compositions of original materials and chemically modified samples. As shown in Fig. 1, after coated with DOPA, a new peak N 1s appeared in wide scan spectra of D-SCPP. It indicated that DOPA, the only compound can introduce nitrogen, reacted with SCPP and formed stable chemical bond between them. The remarkable decrease of Ca and P relative contents along with substantial increase of C content also indicated successful DOPA coating. Besides, it was further demonstrated by following appearances: the [O]/[C] ratios of D-SCPP surface was arranged from 0.1 to 0.13, which was in accordance with theoretical values for DOPA (0.125). Subsequent to modification operation, the certification of SF being attached on the scaffolds was supported by three intense characteristic peaks exhibited at 531, 400 and 285 eV which were respectively attributed to O1s, N1s and C1s while peaks of Ca and P disappeared. Furthermore, compared with D-SCPP scaffolds, the [O]/[C] ratio of SCPP/D/SF increased to 0.3, which was very close to theoretical value for SF molecule [19, 31]. Consequently, after successful introducing DOPA and sequentially modifying D-SCPP by SF, SCPP/D/SF was obtained and achieved some excellent properties. SEM observations in Figure S2 also certified DOPA's successful coating, which was in according with the result in XPS.

3.2 Biomechanical examination

SF-coating on D-SCPP scaffolds would be conductive to eliminating fragility of initial SCPP material, providing scaffolds with better biomechanical strength and longer support for new tissue formation[32]. Table 1 showed compressive and impact strength of scaffolds prepared in this work. As shown, the compressive strength of initial SCPP scaffolds was 2.38 MPa, which was slightly higher than that of D-SCPP samples. It may be attributed to continuously self-degradation of DOPA in alkaline solution, which was proved in degradation test in **Figure S4**. At the same time, a slight difference was discovered in impact strength test. The notched impact strength of D-SCPP is slight higher than that of SCPP group, which may because of DOPA coating played some part in preventing cracks propagated to larger ones. As confirmed in Fig. 2(B), a massive of small cracks are distributed in the whole D-SCPP scaffold but no large fatigue cracks are observed. Stress can be effectively transferred from matrix to these small cracks to avoid debonding during the corresponding impact strength increased. On the contrary, the cracks on SCPP scaffold propagated rapidly without prevention. These overlarge cracks accelerated the fracture of scaffold and its impact strength decreased to some extent.

While, after D-SCPP scaffolds were further modified by coating SF, the compressive strength of scaffolds dramatically enhanced from 2.38 to 3.05 MPa and approximatively 1.3 times' increase of impact strength for SCPP was reached after DOPA/SF modification. Based on values above, it was obvious that the increment of strength depended largely on the presence of DOPA-SF coating. This phenomenon might be owning to following reasons. SF coating enlarged the stress area and shared partial load, thus resulting in improvement of stress condition of scaffolds. Organic and inorganic phases could combine with each other tightly through chemical bond

Table 1. Mechanical properties of SCPP, D-SCPP, SCPP/D/SF and SCPP/GA/SF scaffolds

Scafold type	compresive strenthes (Mpa)	inpact strenth (kJ/m^2)
SCPP	2.38±0.43	6.02±0.55
D-SCPP	2.12±0.53	6.24±0.78
SCPP/D/SF	3.05±0.65*	7.91±0.35*
SCPP/GA/SF	2.43±0.54	---

* means $P < 0.05$ compared with original SCPP scaffold

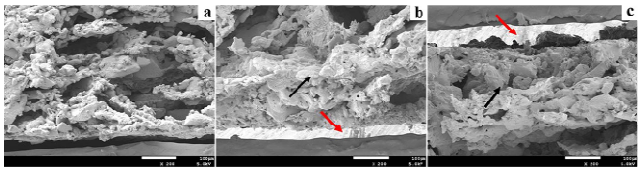

Fig. 2(A) Cross section SEM images of scaffolds (a) D-SCPP, (b) SCPP/D/SF, (c) SCPP/GA/SF. Red arrow: SF; black arrow: SCPP

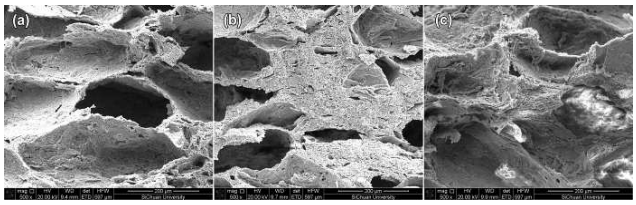

Fig. 2(B) SEM images of scaffold impacted surface (a) SCPP, (b) D-SCPP, (c) SCPP/D/SF.

due to DOPA. Therefore, it prevented the diffusion of cracks in SCPP phases and made scaffolds resist multiple cracking events before totally collapsed. SEM micrographs of impact fracture surfaces were showed in Fig. 2(B). As exhibited, no cracks exist even on the thinnest boundary because of excellent interfacial compatibility between organic and inorganic phases, as well as high ductility SF possessed. Besides, there were some fibril connected through pores, this kind of structure could effectively absorbed fracture energy and prevent propagation of crack. SF could also adhere to SCPP through crosslinking with GA to form network structure and physically encased inorganic materials. As comparison, after coating SF by GA crosslinking, scaffolds exhibited a slight increment in compressive strength compared with original SCPP scaffolds, but significantly lower than that of SCPP/D/SF scaffolds (the impact strength of SCPP/GA/SF was hard to be measured for easily debonding when fixed it by clamps). This may be due to following reasons: the network structures formed by Schiff's crosslinking only physically encased the original scaffolds to restrain frangibility, no stable chemical bonds existed between organic and inorganic phases, thus, phase separation happened easily and their compressive strength decreased[33]. This speculation was predominately confirmed by cross section SEM images. Fig. 2(A) exhibited the cross-sectional SEM images of various scaffold-samples, in SCPP/GA/SF scaffolds, obvious small crack chinks can be observed between SCPP and network structure formed by GA/SF. In contrast, after DOPA being introduced, D-SCPP connected with SF tightly and there was no phase separation happened between them. This phenomenon was exactly in accordance with the result obtained in biomechanical examination and can be used to explain why the compressive strength of SCPP/D/SF scaffolds was more effectively improved[12]. Therefore, introducing DOPA to connect SCPP and SF was selected as optimal method in our researches for avoiding phase separation and eliminating the fragility of original inorganic materials.

3.3 Molecular dynamics simulation

There were a large number of active amino groups in SF molecule that can easily react with DOPA to form tightly adhesion. However, the detailed mechanism of how DOPA molecules attach to inorganic surface was still unknown. Adhesion between DOPA and SCPP was the basic of this study, here we took CPP crystal lattice to replace SCPP in simulation since Sr possessed similar atomic structure to Ca[4]. In view of partial DOPA could be easily oxidized, dopamine and dopaquinone were considered as two possible compound forms. Simulation snapshot was shown in Fig. 3: the simulation box included a CPP slab in its bottom surface (corresponds to a-quartz [001] surface) and an individual relaxation unit cell of DOPA embedded in any possible position of CPP simulation. As could be seen, boundaries in some directions were periodic and large enough box dimensions were necessary in design to avoid interactions between mirror solutes. The snapshot of ultimate simulation state exhibited equilibrated conformation of DOPA in two possible forms with minimum free energy. As revealed in Fig. 3 (B), the hexagonal rings of dopaquinone were easier to lay flatly and closely on the mineral surface than that of DOPA, which promoted adhesion-strength significantly. The reason for this might be that quinone connected to the hexagonal rings featured massive hydrogen bonding interactions and coordination-bonding interaction with CPP surface, which was stronger than pure Van der Waals interactions and promoted adhesion-strength significantly. On the contrary, the hexagonal rings of dopamine were distributed on CPP surface randomly. Therefore, dopaquinone was the primary form of DOPA to interact with mineral surface. Furthermore, as shown in table.2, the interactions of DOPA and CPP were expressed through comparing initial atomic van der Waals radius (H 1.10Å, O 1.52Å, C 1.61 Å and Ca 1.97Å, respectively in theoretical value) with ultimately measured bond lengths. According to the data mentioned above, carbons on the benzene ring of DOPA had delocalized electrons, it could build strong interaction with oxygen atoms in CPP induced by electrostatic force. O atom on catechol formed coordination complexes with Ca2+ ion also contributed to adhesion. In a word, in addition to hydrogen bond, electrostatic force and coordination were also synergistic interactions to make DOPA adhere to SCPP surface tightly.

Table.2 Interaction of DOPA/CPP

Bonding type	Length (Å)	Essential
C-O	3.146	Electrostatic
Ca-O	2.654	Coordination
O-H	1.688	Hydrogen bond

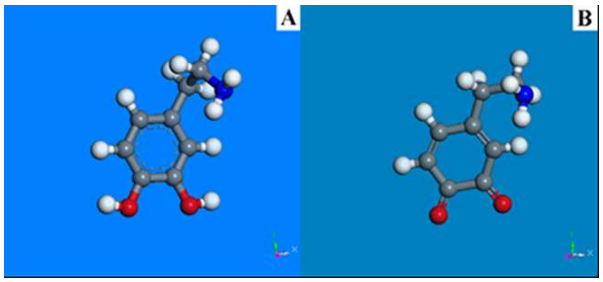

Fig. 3 (A) Two forms relaxation unit cells of DOPA (A: dopamine; B: dopaquinone)

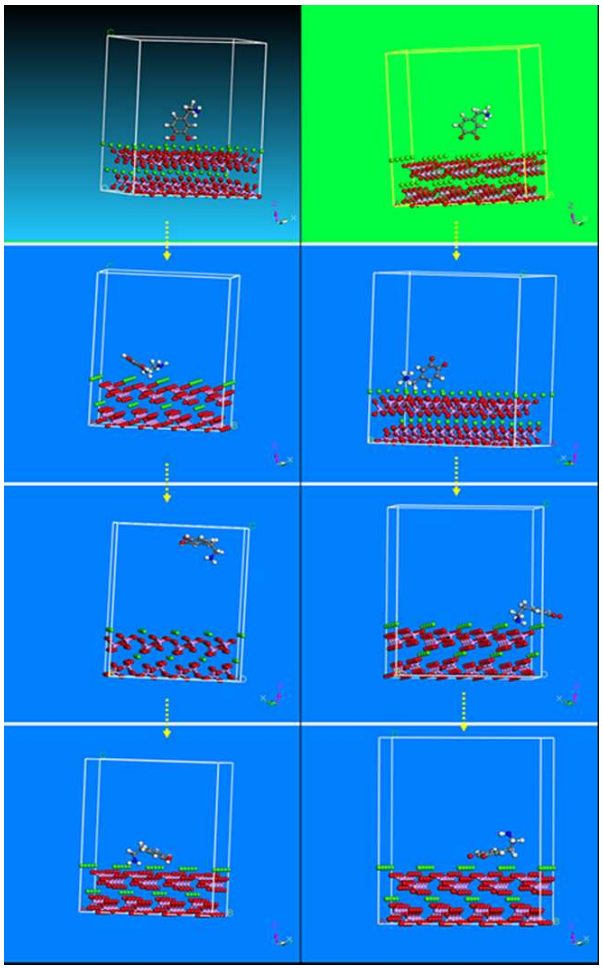

Fig. 3 (B) Orbit of DOPA on CPP (left: dopamine/CPP; right: dopaquinone/CPP)

3.4 Cell proliferation on various scaffolds

The viability of HUVECs and/or MG63 cultured on SCPP, D-SCPP and SCPP/D/SF scaffolds were all determined by MTT assay. HUVECs and/or MG63 directly cultured in DMEM without scaffold were served as blank control for each group. SCPP/GA/SF samples unfortunately failed to serve as positive control in this cell experiment due to rapid fragmentation. The proliferation histograms of test groups were exhibited in Fig. 4 (A) and (B), respectively. As shown in Fig.4 (A), the proliferation of HUVECs cultured on scaffolds increased in all experimental groups during culture period compared with blank control, which indicated both SCPP itself and its modification (functionalized by DOPA or DOPA/SF) could promote growth and proliferation of HUVECs effectively. However, its proliferation rate didn't change significantly after coating DOPA. That may be due to that DOPA could induce the expression of antioxidative enzyme heme oxygenase-1 (HO-1) in cultured endothelial cells, which could just enhance the protection of endothelial cells from damage but behaved no proliferation effect on it[34]. Whereas, after D-SCPP was further modified by coating SF, proliferation of HUVECs cultured on SCPP/D/SF scaffolds increased significantly. As well known, exact nature and function of proteins were determined by the amino acids constructed it. SF is mainly composed of glycine, alanine and serine, it contains peptide sequence structure similar to RGD tripeptide. RGD tripeptide was a tripeptide consist of arginine, glycine and aspartic acid, which could effectively promote cells proliferation, adhesion, migration and differentiation. So, with identical cytocompatibility of RGD, SF could also stimulate HUVECs' growth and proliferation effectively[35, 36]. Analogous conclusion was obtained in SEM observation in **Figure S5**.

Those scaffolds accelerated MG63 growth with analogous trend. However, unlike DOPA showing no stimulation for HUVECs' proliferation, noticeable elevation of adhesion and growth of MG63 on DOPA-coated SCPP was shown in Fig.4 (B), which was in accordance with the result reported by Tsai [37, 38]. SCPP/D/SF, the further modified scaffolds by SF showed more excellent performance than D-SCPP. Therefore, promising potential application of SCPP/D/SF scaffold in bone tissue engineering was further demonstrated by its excellent cytocompatibility.

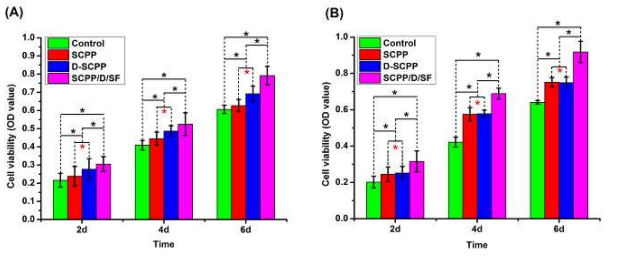

Fig. 4 Cell viability of (A) HUVECs and (B) MG63 cultured with different scaffolds; * means the difference attained a statistically significant increase compared with each other2.5 Cell distribution and morphology

3.5 Cell distribution and morphology

To get a clear vision of cells ingrowth inside the porous scaffolds, confocal laser scanning microscopy (CLSM) was employed. Growing states of MG63 and HUVECs cultured on original or modified SCPP scaffolds were observed by CLSM after labelling cytoskeleton with FITC and dyeing nucleus with DAPI. FITC could react with molecules containing amino groups and form green fluorescent substance, whereas DAPI would turn to bright blue selectively when it bound to double stranded DNA. As exhibited in Fig.5, HUVECs and MG63 grew well on the surface of original SCPP, D-SCPP as well as SCPP/D/SF scaffolds. Cells spanned between adjacent pores,

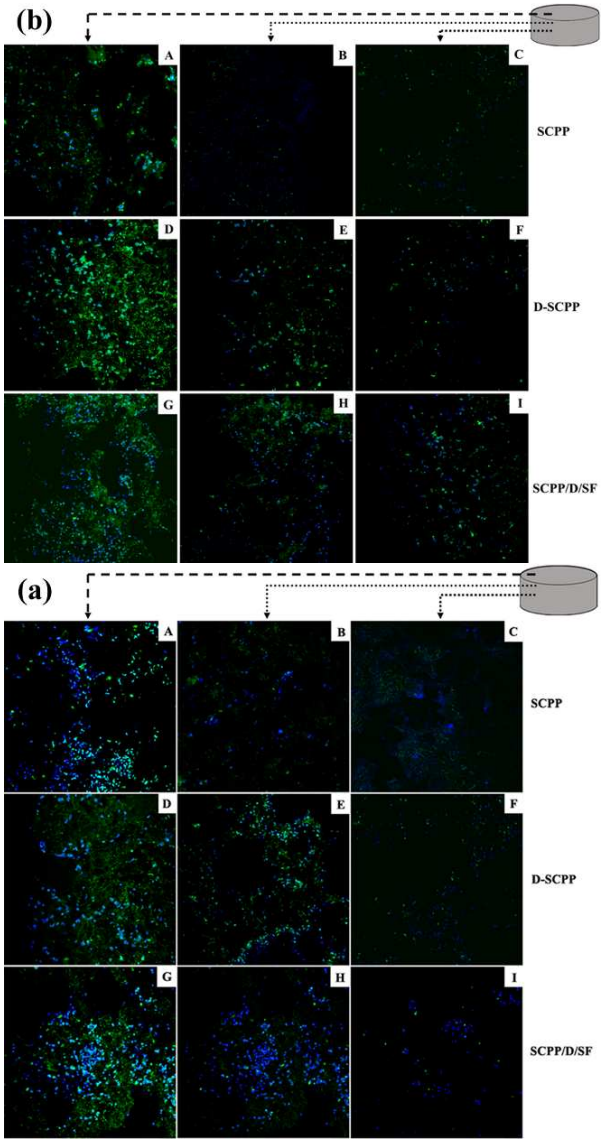

Fig.5 CLSM images of (a) HUVECs and (b) MG63 cultured with different scaffolds.

yielding a high accumulation density of adherent cells. After D-SCPP samples further modified by coating SF, cells were approximatively spread over the whole surface, which indicated that DOPA-SF coating could stimulate cell-proliferation. Inside the materials, there were almost no cells observed in the center of SCPP or D-SCPP scaffolds, but there were still a significant quantity of cells inside SCPP/D/SF although with a dramatic decrease, somewhat proving that more cells had a tendency to distribute inside scaffolds and appeared to bridge over its pores after further modified by coating SF. It also suggested that DOPA-SF coating could induce cells migrating towards interior of scaffold without impairing its porous structure. Generally, the sizes of green fluorescent area were proportional to the cytoactivity and cell number in CLSM method. Being contrary to this common sense, the large green fluorescent area appeared in D-SCPP scaffold in this study did not indicate an acceleration of cells proliferation by initial DOPA modification[34]. This might because that in addition to cytoplasm or cytoplasm matrix, FITC could also react with other substance containing amino groups (such as DOPA and SF) and form green fluorescent substance. As a result, SCPP/D/SF scaffold presented a good potential to be bone regeneration material: along with effectively stimulating cells proliferation, it could induce cells migrating towards interior of scaffolds through the pores, which was exactly in accordance with the result in MTT test. Especially to deserve to be mentioned, even inside SCPP/D/SF scaffold, the quantity of cells decreased dramatically. We inferred that cells reduction was not caused by the concentration of SF turned lower inside scaffold. It has been proved by EDS measurement. As exhibited in Figure S3, there is no significant deviation of chemical compositions between interior and exterior of scaffold. Therefore, the dramatically reduction of cells number inside SCPP/D/SF scaffold may be caused by lacking of oxygen and other nutrient substance.

3.6 Alkaline phosphatase (ALP) activity and mineralization analysis

The effect of DOPA/SF coating on osteoblasts' maturation was determined by alkaline phosphatase (ALP) activity in MG-63 cell because their maturation can increase alkaline phosphatase activity correspondingly. As exhibited in Fig. 6(A), the ALP activity of MG63 cultured on scaffolds increased in all experimental groups during culture period. Both DOPA and DOPA/SF modification can effectively promote the increasement of ALP activity. Especially, when cells were incubated with SCPP scaffolds in the presence of DOPA/SF, the stimulatory effect of SF on ALP activity was significantly increased, which indicated its excellent osteogenic property. This result was also confirmed by Alizarine Red-S staining data. In Fig. 6 (B), cells were stained by alizarin red to determine the formation of calcium nodules due to mineralisation.[39] After 7 days' culture, several areas positive for calcium were observed around SCPP/D/SF scaffold, while it appeared in SCPP and D-SCPP groups after 10 d. Moreover, in the SCPP scaffold, calcium deposits were larger than in other ones, which further proved that DOPA/SF modification could effectively improve the osteogenic property.

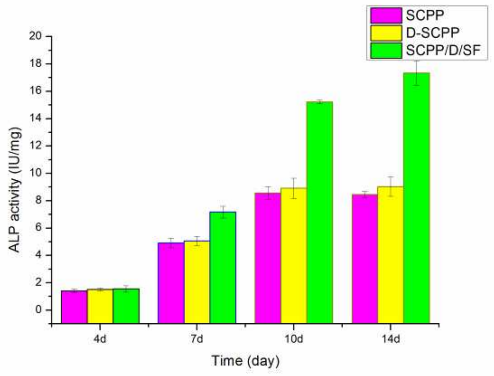

Fig. 6 (A) Alkaline phosphatase activity of MG63-cells on scaffolds with after 4, 7, 10 and 14 days of culture

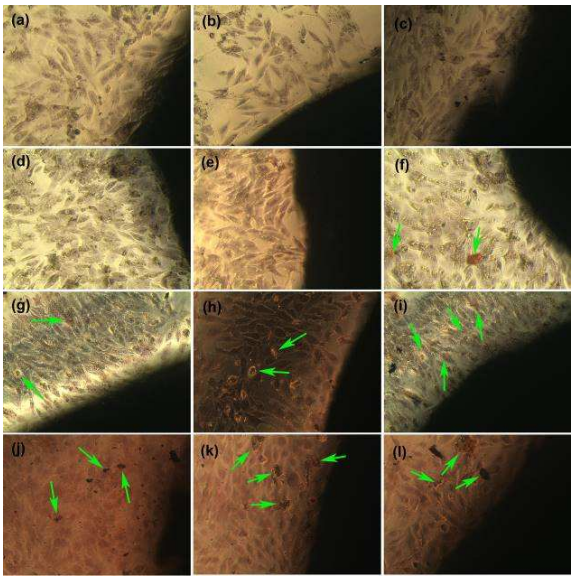

Fig. 6(B) Alizarin redstaining of scaffolds on day 4 (a-c), day 7 (d-f), day 10 (g-i), day 14 (j-l); SCPP (a, d, g, j), D-SCPP (b, e, h, k), SCPP/D/SF (c, f, i, l), respectly. Green arrows: calcium nodules

3.7 Measurement of VEGF and bFGF

VEGF and bFGF are two potent angiogenic growth factors with ability to stimulate cell-proliferation and cell-migration. Meanwhile, they could also induce vascularization process or mineralization of matrix calcium[38,40]. As an effective method to detect trace amount of cytokine, ELISA was used in our study to quantificationally evaluate the levels of those two angiogenic growth factors.

As presented in Fig. 7, in SCPP/D/SF group, the amount of VEGF or bFGF was all higher than that in SCPP and D-SCPP groups, both co-culturing with HUVECs and with MG63. We inferred that this phenomenon may be related to following reasons: DOPA-SF coating could effectively stimulate cells proliferation, thus there were more cells secreting VEGF and bFGF on scaffolds than that on SCPP or D-SCPP. In addition, DOPA-SF

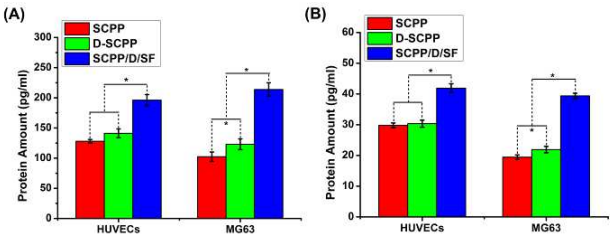

Fig.7 The effect of various scaffolds on cellular (A) VEGF and (B) bFGF secretion (* means the difference attained a statistically significant, $p<0.05$)

coating on the surface could provide a more suitable environment for cells growth due to that its component was similar to extracellular matrix, which not only promoted cell proliferation and adhesion, but also stimulate VEGF and bFGF secretion. In Fig. 7(A), the amounts of VEGF secreted from both HUVECs and MG63 on D-SCPP were higher than that in SCPP group. That was largely due to that DOPA introduction slightly promoted cells proliferation (more obvious effect was observed on MG63), and thus stimulated VEGF secretion. Similar phenomenon was exhibited on bFGF secretion. However, as shown in Fig. 7(B), no statistically significant differences could be found in the level of bFGF secreted from HUVECs between SCPP and D-SCPP group. This might because SCPP could only stimulate bFGF secretion in a very low level (only reached 20% of VEGF), slight proliferation of HUVECs was not adequate to affect bFGF secretion totally[41]. All data mentioned above forcefully demonstrated SCPP/D/SF could effectively promote the secretion of VEGF and bFGF, it had a promising potential to employ as scaffold material for bone tissue engineering.

3.8 Histological observation and immunohistological assessment

After operation, no infection or inflammation were shown in implantation sites of rabbits. Histological and immunohistological photographs of excised specimens were exhibited in Fig.8, where both tissue response and scaffolds degradation could be observed. HE staining analysis in Fig.8 (B) presented that in SCPP/D/SF group there were no inflammatory responses in peripheral region of scaffolds and less fibrous tissues around materials were observed. In addition, along with new bone in margin, a large quantity of newly formed bone tissues with osteotylus and trabecular structure were distinctly observed in the center. In contrast, only sporadic new bone was observed in center of scaffold and some inflammatory cells were found surrounding scaffolds in SCPP group. There was no obvious promotion in biocompatibility but the antidegradation ability intensified to some extent after DOPA-modification. The degradation of D-SCPP was mild or even absent after a period of time. The result of HE stain indicated that DOPA-SF coating could effectively accelerate mineralization process and new bone regeneration.

Immunohistological stain was employed to evaluate expression of angiogenetic growth factor (VEGE and bFGF) in scaffolds. As presented in Fig. 8(B), after implantation for 8 weeks, the positive immunohistochemistry staining for VEGF and bFGF was observed in newly regenerated tissue in all groups. Especially, more intensive positive staining was predominantly accomplished in SCPP/D/SF group. 12 weeks later, the intensity positive immunohistochemistry staining for VEGF and bFGF still maintained in SCPP/D/SF group, whereas it decreased in SCPP or D-SCPP groups. Therefore, DOPA-SF coating could not only promote new bone formation but also enhance VEGF and bFGF secretion from host cells. Meanwhile, Figure S6 presented result of bone mineral density test which was aimed to determine the accurate quantification of newly formed bone. It further proved that SCPP/D/SF could promote the formation of new bone effectively.

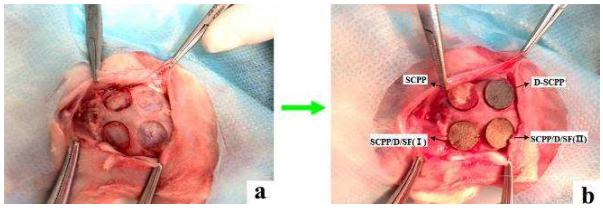

Fig.8 (A) Photographs of In vivo animal molding. Defects on crinial bone (a) and (b) materials implanted

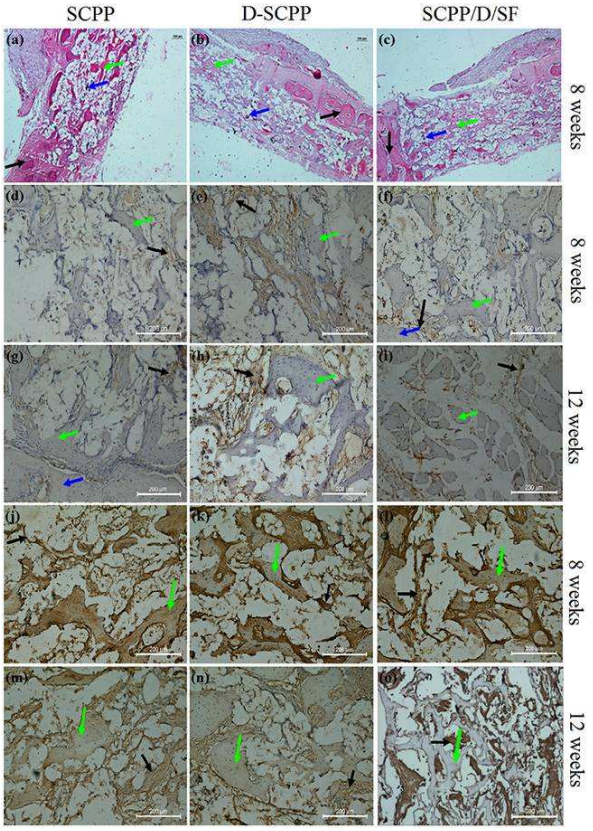

Fig. 8(B) The HE stain (a-c) and the immunohistochemical analysis by VEGF staining (d-i) and bFGF-staining (j-o) on the new bone tissues after implantation in rabbits for predetermined period (HE: (a) SCPP, (b) D-SCPP and (c) SCPP/D/SF; VEGF: (d, g) SCPP, (e, h) D-SCPP and (f, i) SCPP/D/SF; bFGF: (j, m) SCPP, (k, n) D-SCPP and (l, o) SCPP/D/SF Black arrow: fibrous capsule; green arrow: new formed bone; blue arrow: host bone

4. Conclusion

In this work, through facile modification by SF coating after introducing DOPA, a novel scaffold material based on original SCPP scaffolds was successfully prepared. This modified process was confirmed by XPS analysis. Molecular dynamic simulation indicated that the oxidized state, dopaquinone, was the primary form of DOPA making it attach to the surface of the CPP (SCPP) scaffold tightly. The driving force of this attachment is the synergistic interaction of hydrogen-bonding, coordination interaction and electrostatic interaction. SCPP/D/SF scaffolds not only possessed significantly higher compressive strength but also obtained better biocompatibility. The results of MTT assay implied it could accelerate the proliferation and adhesion of HUVECs and MG63. Meanwhile, observed by CLSM, DOPA-SF coating could also induce cells migrating towards interior of scaffolds' pores, which is an ideal and essential feature of bone scaffold materials for clinical application. In addition, SCPP/D/SF scaffolds could stimulate secretion of VEGF and bFGF from seeded cells according to the results of ELISA assay. In vivo animal experiment, histological examination showed that SCPP/D/SF scaffolds could effectively accelerate mineralization process and new bone regeneration, while immunohistological assessment indicated the novel scaffolds could not only promote new bone formation but also enhance VEGF and bFGF secretion from host cells, which confirmed the results of the ELISA assay. In conclusion, SCPP/D/SF is a novel scaffold material with excellent physicochemical properties and biocompatibility, especially the ability to promote the process of osteogenesis and vascularization, presented an excellent potential as bone regeneration materials for clinical application.

Acknowledgments

This work was supported by two National Natural Science Foundation of China (51503129 and 30870616), the Scientific and technological project of Sichuan Province (2012SZ0015) and the Scientific and technological project of Chengdu (2014-HM01-00207-SF).

Notes and references

1 S. R. Esfahani, F. Tavangarian and R. Emadi, Mater. Lett., 2008, 62, 3428-3430.
2 R. Pilliar, M. Filiaggi, J. Wells, M. Grynpas and R. Kandel, Biomaterials, 2001, 22, 963-972.
3 Z. Gu, H. Xie, L. Li, X. Zhang, F. Liu and X. Yu, J. Mater. Sci. Mater. Med., 2013, 24, 1251-1260.
4 K. Qiu, X. J. Zhao, C. X. Wan, C. S. Zhao and Y. W. Chen, Biomaterials, 2006, 27, 1277-1286.
5 R. M. Pilliar, R. A. Kandel, M. D. Grynpas and Y. Hu, J. Biomed. Mater. Res., Part B, 2013, 101, 1-8.
6 E. Wenk, H. P. Merkle and L. Meinel, J. Controlled Release, 2011, 150, 128-141.
7 R. E. Marsh, R. B. Corey and L. Pauling, Biochim. Biophys. Acta, 1955, 16, 1-34.
8 Y. Wang, H.-J. Kim, G. Vunjak-Novakovic and D. L. Kaplan, Biomaterials, 2006, 27, 6064-6082.
9 A. Vasconcelos, G. Freddi and A. Cavaco-Paulo, Biomacromolecules, 2008, 9, 1299-1305.
10 S.-S. Kim, M. S. Park, O. Jeon, C. Y. Choi and B.-S. Kim, Biomaterials, 2006, 27, 1399-1409.
11 B. M. Chesnutt, Y. Yuan, K. Buddington, W. O. Haggard and J. D. Bumgardner, Tissue Eng., Part A, 2009, 15, 2571-2579.
12 A. J. Salgado, O. P. Coutinho and R. L. Reis, Macromol. Biosci., 2004, 4, 743-765.Orthod.
13 S. He, C. Scott and P. Higham, Biomaterials, 2003, 24, 5045-5048.
14 Y. Yin, F. Ye, J. Cui, F. Zhang, X. Li and K. Yao, J. Biomed. Mater. Res., Part A, 2003, 67, 844-855.
15 Q. Ye, F. Zhou and W. Liu, Chem. Soc. Rev., 2011, 40, 4244-4258.

16 P. Roach, T. Parker, N. Gadegaard and M. Alexander, Surf. Sci. Rep., 2010, 65, 145-173.
17 W. O. Yah, H. Xu, H. Soejima, W. Ma, Y. Lvov and A. Takahara, J. Am. Chem. Soc., 2012, 134, 12134-12137.
18 J. J. Wilker, Nat. Chem. Biol., 2011, 7, 579-580.
19 H. Lee, S. M. Dellatore, W. M. Miller and P. B. Messersmith, science, 2007, 318, 426-430.
20 Z.-Y. Xi, Y.-Y. Xu, L.-P. Zhu, Y. Wang and B.-K. Zhu, J. Membr. Sci., 2009, 327, 244-253.
21 L.-P. Zhu, J.-Z. Yu, Y.-Y. Xu, Z.-Y. Xi and B.-K. Zhu, Colloids Surf. B. Biointerfaces, 2009, 69, 152-155.
22 J.-H. Jiang, L.-P. Zhu, X.-L. Li, Y.-Y. Xu and B.-K. Zhu, J. Membr. Sci., 2010, 364, 194-202.
23 J.-H. Jiang, L.-P. Zhu, X.-L. Li, Y.-Y. Xu and B.-K. Zhu, J. Membr. Sci., 2010, 364, 194-202.
24 A. L. Cheung, Current protocols in microbiology, 2007, A. 4B. 1-A. 4B. 8.
25 R. H. Kröger and H.-J. Wagner, J. Neurosci. Methods, 1998, 84, 87-92.
26 Y. Nancharaiah, V. Venugopalan, S. Wuertz, P. Wilderer and M. Hausner, J. Microbiol. Methods, 2005, 60, 179-187.
27 H. Puchtler, S. N. Meloan and M. S. Terry, J. Histochem. Cytochem., 1969, 17, 110-124.
28 J.-H. Byun, B.-W. Park, J.-R. Kim and J.-H. Lee, Int. J. Oral Maxillofac. Surg., 2007, 36, 338-344.
29 H. Xie, J. Wang, C. Li, Z. Gu, Q. Chen and L. Li, Ceram. Int., 2013, 39, 8945-8954.
30 D. Pacicca, N. Patel, C. Lee, K. Salisbury, W. Lehmann, R. Carvalho, L. Gerstenfeld and T. Einhorn, Bone, 2003, 33, 889-898.
31 H.-J. Jin, J. Park, R. Valluzzi, P. Cebe and D. L. Kaplan, Biomacromolecules, 2004, 5, 711-717.
32 G. Uzun, N. Hersek and T. Tincer, J. Prosthet. Dent., 1999, 81, 616-620.
33 Q. Wu, X. Zhang, B. Wu and W. Huang, Mater. Lett., 2013, 92, 274-277.
34 S. P. Berger, M. Hünger, B. A. Yard, P. Schnuelle and F. J. Van Der Woude, Kidney Int., 2000, 58, 2314-2319.
35 J. L. Wang, K. F. Ren, H. Chang, F. Jia, B. C. Li, Y. Ji and J. Ji, Macromol. Biosci., 2013, 13, 483-493.
36 Y. Kaneshita, S. Goda and T. Kawamoto, Orthodontic Waves, 2007, 66, 122-128.
37 W.-B. Tsai, W.-T. Chen, H.-W. Chien, W.-H. Kuo and M.-J. Wang, J. Biomater. Appl., 2014, 28, 837-848.
38 Y.-Q. Yang, Y.-Y. Tan, R. Wong, A. Wenden, L.-K. Zhang and A. B. M. Rabie, Int. J. Oral Sci., 2012, 4, 64-68.
39 Y.-S. Cho, W.-K. Jung, J.-A. Kim, I.-W. Choi and S.-K. Kim, Food chemistry, 2009, 116, 990-994.
40 H.-P. Gerber, V. Dixit and N. Ferrara, J. Biol. Chem., 1998, 273, 13313-13316.
41 M. S. Park, S. S. Kim, S. W. Cho, C. Y. Choi and B. S. Kim, J. Biomed. Mater. Res., Part B, 2006, 79, 353-359.

Graphical Abstract